Experimental investigations into vortex flow in a straight, annular section channel

R. Bettocchi and G. Cantore*

Results of experimental velocity measurements in air at several cross-sections along a straight annular section channel comparable to a hydraulic machine admission duct are presented. The flow analysis focusses on the axial and tangential velocity components and their modification with changes in the intensity of swirl along the channel. Particular prominence is given to an anomalous flow, the 'dead water core', occurring at the greatest swirl intensities. An earlier method[1] of evaluating the core size of this anomalous flow on the basis of a vortex-type schematization is tested; Strscheletzky's method[2] is also analysed. Finally a definition of the dead water core dimensions based on the axial velocity component distribution is proposed

Keywords: *turbines + hydraulic, vortices, swirl, dead water core*

This study is related to a previous experimental analysis of the flow in a straight, circular cross-section channel downstream of a cylindrical guide vane[1]. That original channel has now been modified by the insertion of a hub to resemble that of a rotorless axial hydraulic helical-type machine (Fig 1).

The flow has been analysed to determine the type of vortex formed in the channel and the diameter of the zone coaxial with the central hub where, due to the small guide vane openings, an anomalous stream is formed. This analysis shows a steep decrease and/or inversion of axial velocity, an almost forced-vortex tangential velocity distribution, and a substantial decrease in total pressure. Formation of this inner core in an axial machine causes a drop in efficiency, affects cavitation, and produces intravane vortices, the cause of vibration[3,4].

Apparatus and experimental method

The test channel is shown in Fig 1, where the cross-sections at which the velocity component distributions were measured are numbered. The hub has a cylindrical section of diameter $D_0 = 150$ mm and is inside a duct of diameter $D = 340$ mm, giving D_0/D as 0.44.

The tests were performed using air with the velocity measurements taken using a five-hole spherical probe. Velocity traversing was undertaken at each cross-section in the duct, at several points, with the axial and tangential velocity components being determined from probe calibration data. The test duct joins a measuring duct having a standard orifice-meter, preceded by a flow straightener, to measure the mean flow rate.

Velocity distributions at the test sections were obtained at values of the vane-angle δ (Fig 1) between 19° and 75°, in a Reynolds number range between 0.7×10^5 and 3.7×10^5.

* Istituto di Macchine, Facoltá Ingegneria, University of Bologna, 40136 Bologna, Viale Risorgimento, n.2, Italy
Received 11 November 1983 and accepted for publication on 25 April 1984

Results

In terms of the ratio r/R, between the generic radius and that of the duct, Figs 2 and 3 show the variation of V_a/V_{am} and V_t/V_{am} respectively obtained at section 2 of the channel (Fig 1). The mean axial velocity V_{am} was obtained from the flow rate obtained by integration across the test section.

Velocity distributions were measured at all sections for various flow rates in the Reynolds number range noted above, taking care to check that the axial and tangential components did not depend on the value of the Reynolds numer, ie that the stream lines did not vary with the Reynolds number. Thus Figs 2 and 3 show the distributions relative to a single flow rate.

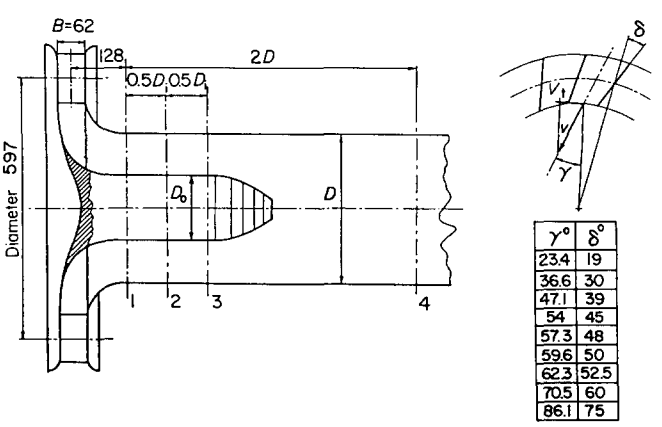

Fig 1 Longitudinal section of the test channel showing angles δ and γ

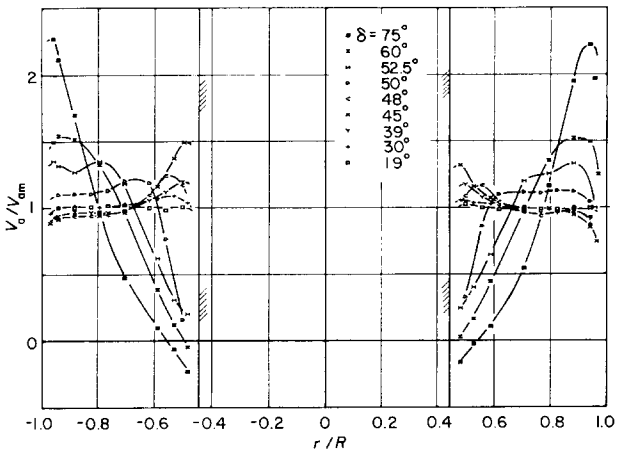

Fig 2 Axial velocity in terms of r/R *for various* δ *angles in section 2 of the test channel*

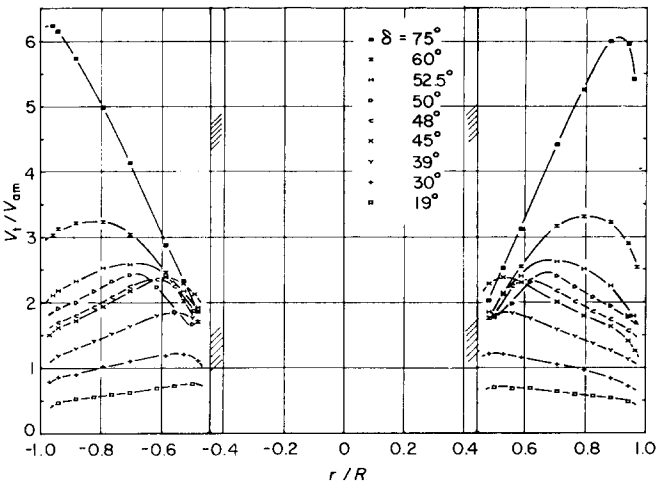

Fig 3 Tangential velocity in terms of r/R *for various* δ *angles in section 2 of the test channel*

Also, Fig 7 shows the axial and tangential velocity component distributions at all test sections for some of the values of δ tested. Reynolds number values of the tests shown in the Figs 2–7 are indicated in Table 1 with corresponding values of δ tested.

Fig 7 completes the presentation of the investigations carried out and was drawn with a view to showing how flow develops along the channel axis, which is discussed later.

Discussion

Effect of the variation of δ *on the flow*

Examination of the velocity ratio plots in Figs 2 and 3 shows how the flow pattern at the section considered is modified by varying δ. For values of δ up to 48°, the tangential velocity component is that of a free vortex over almost the entire section of the channel while the axial component remains practically unchanged, except for some cases where it increases slightly near the hub wall.

For values of δ above 48°, the free-vortex tangential component distribution affects the outer annular region. This effect reduces as δ increases, being replaced in the coaxial central hub core by a nearly forced-vortex distribution. The axial velocity component is still almost uniform in the outer annular region, where the tangential component assumes free-vortex distribution; in the coaxial hub core, however, it decreases considerably, reaching zero or negative values near the hub wall.

In essence, for values of δ above 48°, an anomalous stream is revealed in the core. The stream increases in size as δ increases and is characterized by the velocity distributions described above.

In the channel being examined, the genesis of the two zones, inner core and outer ring, marked by distinctly different axial and tangential velocity component distributions, is the same as that found in the same channel without the hub[1]. Figs 4–6, for values of δ of 30°, 45° and 52.5° respectively, compare the axial and tangential velocity distributions in the two channels, with and without the hub, at section 1. For the hubless channel, the velocity distributions were compared by calculating the mean axial velocity with reference only to the flow rate passing through the outer ring, equal in area to that of the hub channel.

These figures show how the presence of the hub tends to 'cut' the inner core crossed by the anomalous stream,

Notation

B	Guide-vane height
D	Duct diameter
D_i	Hydraulic diameter of the annular section, $D-D_0$
D_0	Hub diameter
K	Momentum flux per unit flow rate
Q	Volume flow rate
r	Radius
R	Duct radius
Re	Reynolds number, $V_{am}D_i/\nu$
r_f	'Dead water' core radius, calculated on the basis of the vortex schematization proposed by the authors
r_m	'Dead water' core radius, calculated on the basis of the schematization proposed by Strscheletzky
V	Velocity
γ	Angle formed at guide-vane exit by the intravane duct mean line and radial direction
Γ	Circulation
δ	Angle formed by the guide vanes and the radial direction passing through the fulcra of the vanes themselves
ν	Kinematic viscosity
ω	Rotation

Subscripts

a	axial
am	mean axial
t	tangential

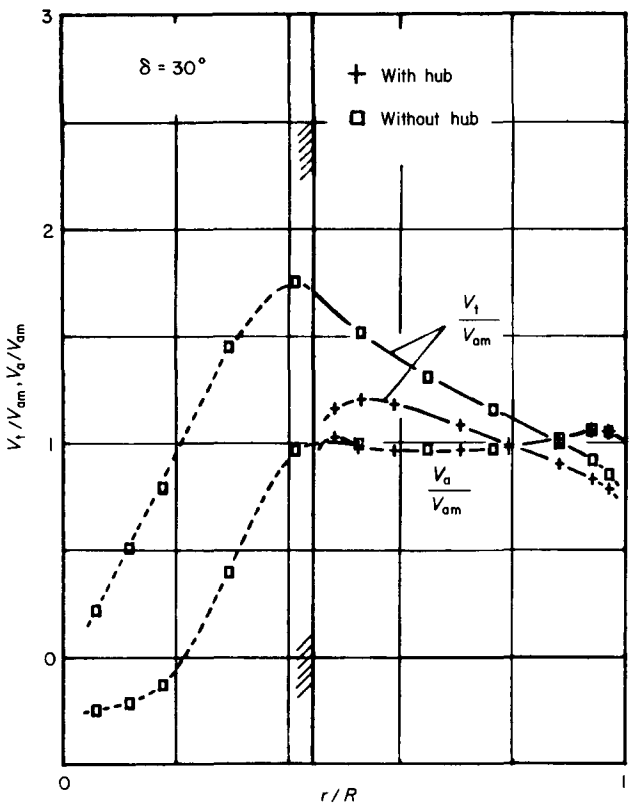

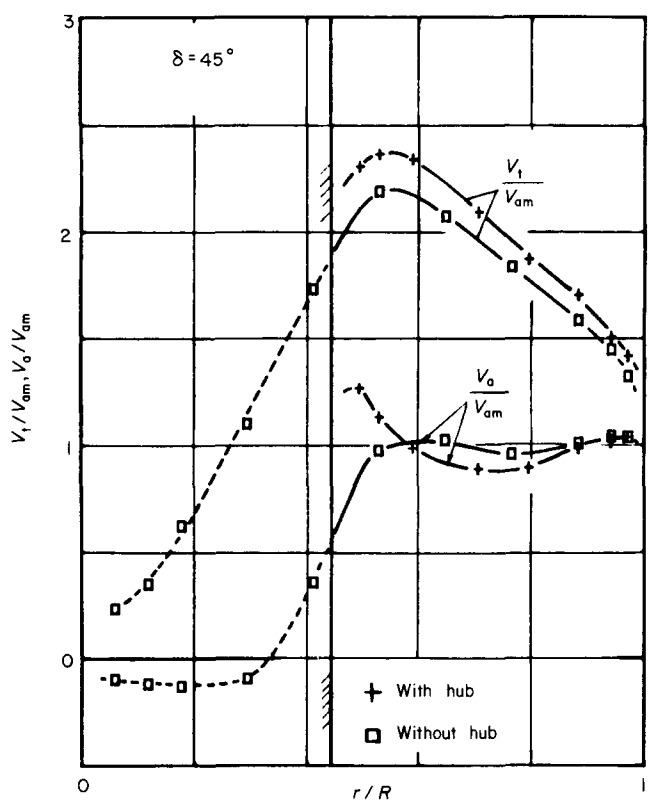

without substantially modifying the velocity distributions in the outer ring surrounding it. In the case in question, hub dimensions for δ equal to 30° and 45°, as seen in Figs 4 and 5, are such that it appears as if the inner core were inside the hub itself.

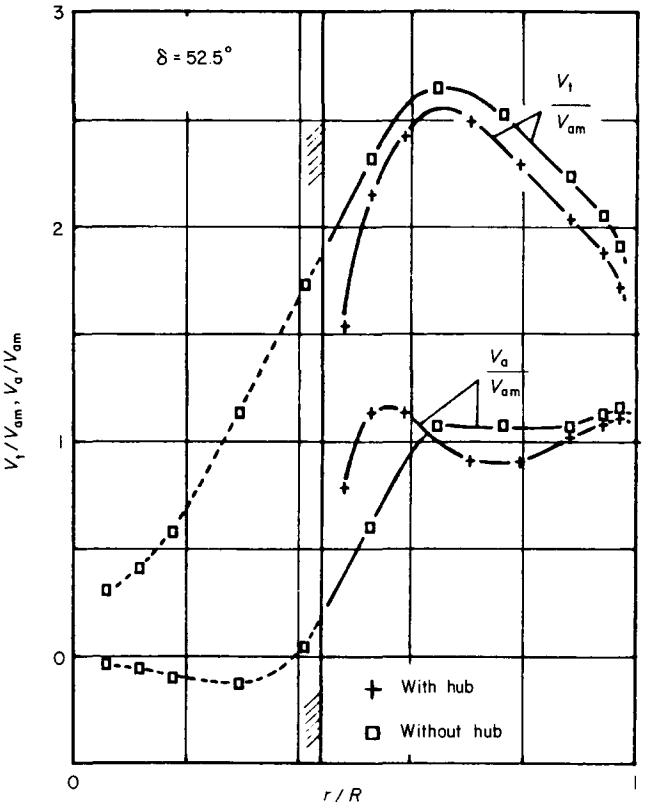

Figs 4 (top left), 5 (lower) and 6 Comparisons between the axial and tangential velocities obtained in the two channels, with and without the hub

Vortex-type schematization

Fig 7, illustrating schematically the test channel, shows the axial and tangential velocity distributions, referred to the mean axial velocity, corresponding to δ values of 30°, 45°, 52.5°, 60° and 75° at test sections 1, 2, 3 and 4, and obtained as the mean of measurements along the two radii of the channel. This shows how the flow along the channel axis alters, in terms of the two velocity components, at the four sections.

The distributions of tangential velocity reported here and those of Fig 3 indicate the possibility of schematizing its variation by a constant rotation forced vortex around the duct axis, which occupies an inner core having radius r_f and a free-vortex in the remainder of the outer ring. Radius r_f of the forced-vortex core, which determines the separation between the two zones affected by the two vortex types, can be calculated from:

$$r_f = (K/\omega)^{1/2} \tag{1}$$

with

$$K = \int_{R_0}^{R} V_t V_a r^2 dr \Big/ \int_{R_0}^{R} V_a r dr$$

In Eq (1), the rotation ω is obtained by extending the tangent from the origin to the V_t curve.

For all those test sections where the existence of an almost forced-vortex is evident, the value of the forced-vortex core radius r_f so calculated is indicated in Fig 7. Note that, in every case, the value of r_f satisfactorily locates the separation between the forced-vortex inner core and the free-vortex outer ring.

Values of r_f at sections 1, 2, 3 and 4 have been

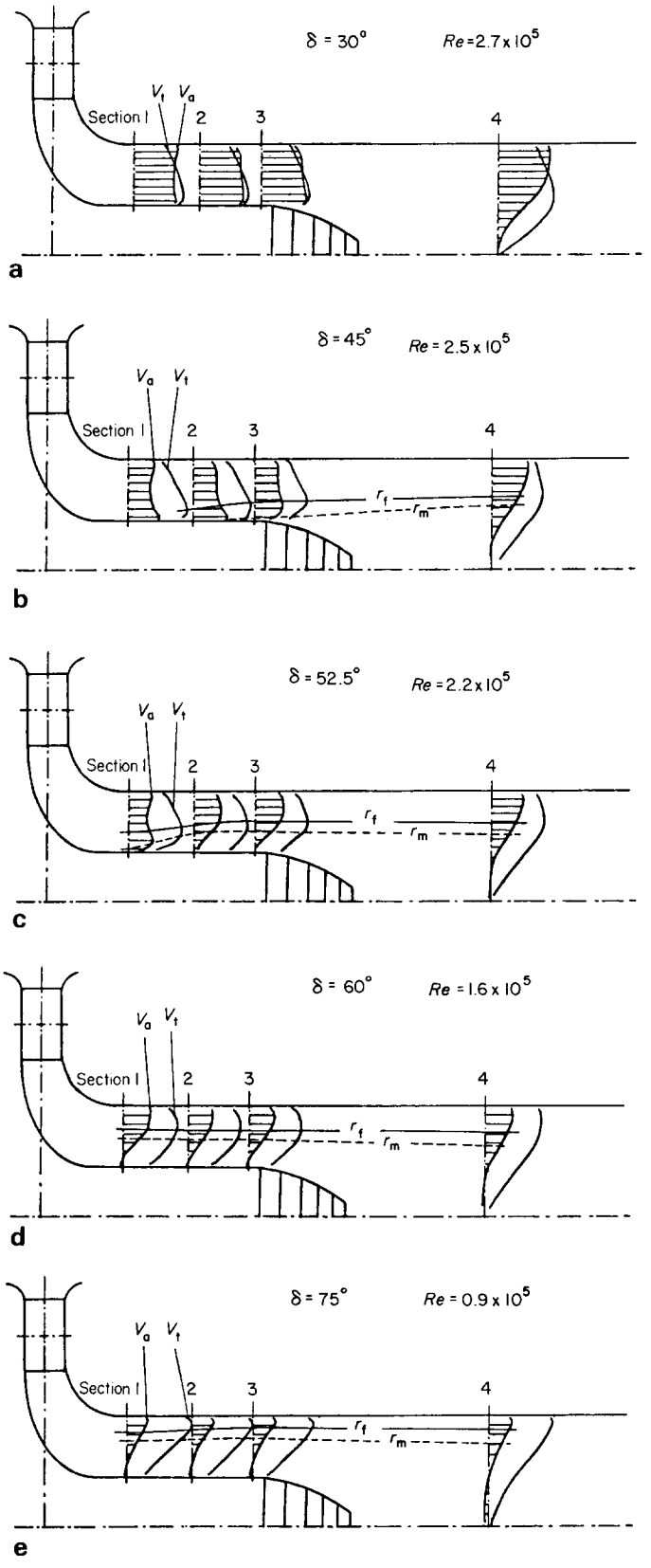

Fig 7 Flow evolution along channel axis

joined in Fig 7 by a continuous line to show how velocity distributions are modified along the channel. Again it is seen that r_f for those test sections where considerable axial velocity reduction is manifested also locates satisfactorily the radius at the sections in which the rapid axial component decrease starts.

As in the previous study for the hubless channel[1], the value of r_f may be assumed to be indicative of the dimensions of the inner core, influenced by the anomalous stream, since it separates both the zones characterized by the two different plots of the tangential components and those with the two different axial plots. From Fig 7(b) it is noted that the anomalous central core begins to form from $\delta = 45°$. Again, it is seen that the size of the anomalous central core increases with δ at the same channel section (Figs 7(b)–(e)).

It should also be noted that the section where the anomalous central core begins moves upstream as δ increases, and that the inner core radius increases downstream till a constant value is reached (see Figs 7(b) and (c)). Finally, for the highest values of δ, that is, for the smallest distributor openings, the core at section 1 has already reached a considerable size which does not change in a downstream direction (see Figs 7(d) and (e)).

Inner core size evaluation

To calculate inner core radius, Strscheletzky[2] proposed a method based on a stepped axial velocity component pattern which assumes a value of zero at the inner core and a constant mean value for the remainder. It is, therefore, as if the flow rate passed only through the outer ring.

This results in the inner core radius r_m given by:

$$\frac{r_m}{R} = \left(1 - \frac{1 - \left(\frac{R_0}{R}\right)^2}{\bar{V}_a / V_{am}}\right)^{1/2} \tag{2}$$

where $\bar{V}_a$ is the arithmetic mean of the velocity values relative to the outer ring. With obvious reference to the axial velocity component distribution pattern, the author calls the inner core, 'dead water'.

r_m was calculated from Eq (2) for all the velocity distributions obtained, using Strscheletzky's method[2], and is plotted in Fig 7 and joined by dashed lines. Note that, in almost all cases reported, the 'dead water' core is better defined by r_f than r_m since this value falls within the radius range where the axial velocity has already begun to decrease. It is, therefore, suggested that r_f is better than r_m in defining the separation between the two zones affected by the two different variations of the tangential and axial velocity components. Nevertheless, by indicating r_m as well as r_f one can, in some cases, better characterize the inner core than with r_f alone.

To compare the present results with the theoretical ones suggested by Strscheletzky[2], the values of r_m/R in Fig 8 are plotted against the $Q/\Gamma R$ parameter. Circulation Γ has been calculated[2] from:

$$\Gamma = 2\pi(\overline{V_t r}) \tag{3}$$

where $(\overline{V_t r})$ is the arithmetic mean of the product $(V_t r)$ relative to the same outer ring as when determining $\bar{V}_a$.

Good agreement is found between the results obtained and curve 'b', which is relative to the case where no vortex destroyer exists downstream of the test section,

Table 1 Test conditions

δ, deg	19	30	39	45	48	52.5	60	75
$Re \times 10^{-5}$	3.7	2.7	3.0	2.5	2.6	2.2	1.6	0.9

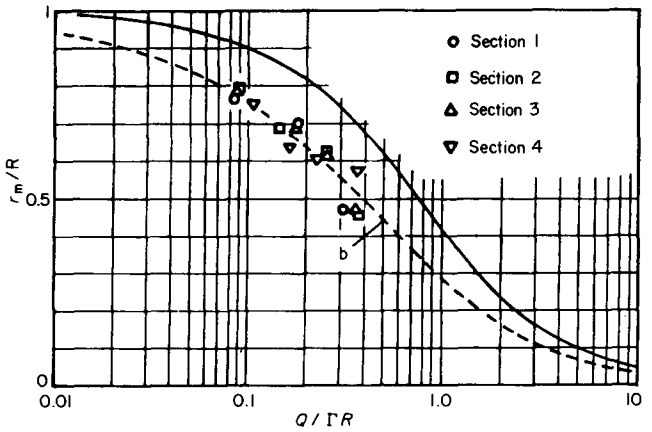

Fig 8 Comparison between Strscheletzky's theoretical curve and the authors' experimental results

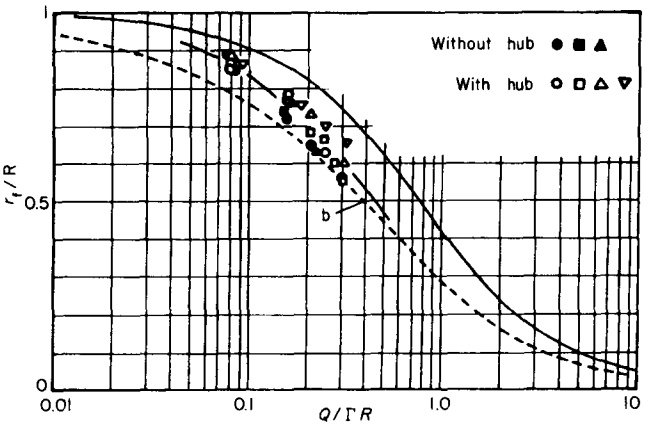

Fig 9 Experimental results compared with Strscheletzky's curve

or is more than three times the hydraulic diameter away from it.

Finally, Fig 9 shows, in the form suggested by Strscheletzky, the values of r_f/R, calculated using Eq (1), relative to the velocity distributions obtained in the channel with the hub for values of $Q/\Gamma R$ below about 0.4; at these values, the 'dead water' inner core was encountered. Fig 9 also shows the values of r_f/R relative to the velocity distributions obtained in the hubless channel, again for values of $Q/\Gamma R$ below 0.4. In this case, unlike the earlier method of Strscheletzky[2], the circulation was calculated from:

$$\Gamma = 2\pi K \tag{4}$$

where K is the vortex constant in the section, calculated as already indicated for Eq (1).

Examination of Fig 9 shows that the experimental values of r_f/R practically fall on a curve, which departs from curve 'b' increasingly with decreasing $Q/\Gamma R$. It is, therefore, suggested that this plot should replace the 'b' curve for the evaluation of the dimensions of the anomalous stream inner core.

Since it is possible to express $Q/\Gamma R$ in terms of the geometric characteristics of the distributor used to give desired pre-rotations to the flow (eg for cylindrical distributors with some simplifying hypotheses, the result is* $Q/\Gamma R = B/R \tan\gamma$), the dimensions of the core affected by the anomalous stream can be evaluated from the distributor geometric characteristics alone by employing the method suggested.

* Supposing a uniform distribution of velocity at the distributor exit and that the angle formed by the flow direction and the radial direction is γ, neglecting the energy losses between the distributor exit and the test section, one obtains:

$$\frac{Q}{\Gamma R} = \frac{2\pi R_{exit} B (V_t/\tan\gamma)}{2\pi (V_t R_{exit}) R} = \frac{B}{R \tan\gamma}$$

Conclusions

The results indicate that, at small distributor openings, in a central core of the tested duct, there occurs an anomalous flow characterized by a steep decrease and/or inversion of the axial velocity, an almost forced-vortex tangential velocity distribution and a considerable decrease in total pressure. In axial turbines, this phenomenon causes an efficiency drop and cavitating vortices, which detach near the hub and pass through the runner in a spiral form, thus causing vibration and noise[4]. An experimental curve which permits evaluation of the radius of the region affected by the anomalous stream from the distributor geometric characteristics and its opening is proposed.

References

1. **Bettocchi R and Cantore G.** Ricerche sperimentali sul flusso in un canale rettilineo di sezione circolare in uscita da un distributore cilindrico. *XXXVII Nat. Congr. A.T.I. Padova, Sept 1982*
2. **Strscheletzky M.** Gleichgewichtsformen der rotationssymmetrischen Strömungen mit konstantem Drall in geraden, zylindrischen Rotationshöhlraumen. *Voiht, Forschung und Konstruktion, Oct 1959*
3. **Eichler O.** Vibration phenomena on hydraulic axial turbines. *IAHR–IUTAM 1979, Karlsruhe*
4. **Bettocchi R., Cantore, G., Magri, L. and Ubaldi, M.** Analyse expérimentale de l'écoulement dans la zone axiale des canaux adducteurs des turbines hélices. *Techn. Comm. of S.H.F., Paris, Nov 1982*